Bone Reports 12 (2020) 100240

Contents lists available at ScienceDirect

Bone Reports

journal homepage: www.elsevier.com/locate/bonr

Case Report

A novel missense COL10A1 mutation: c.2020G > A; p. Gly674Arg linked with the bowed legs stature in the Schmid metaphyseal chondrodysplasia-affected Chinese lineage

Qiong Chen[a], Sheng-Nan Wu[a], Yong-Xing Chen[a], Selvaa Kumar C.[c], Lu Zhang[b], Hai-Yan Wei[a,*], Senthil Arun Kumar[a,*]

[a] Department of Endocrinology and Metabolism, Henan provincial key laboratory of children's genetics and metabolic diseases, Henan children's hospital (Children's hospital affiliated to Zhengzhou University), No-33, Longhu Waihuan East road, Zhengzhou 450018, China
[b] Shanghai We-Health Biomedical Technology Co. Ltd, Shanghai 201315, China
[c] School of Biotechnology and Bioinformatics, D. Y. Patil Deemed to be University, Sector-15, CBD Belapur, Navi Mumbai 400614, India

ARTICLE INFO

Keywords:
Schmid metaphyseal chondrodysplasia
COL10A1 mutation
Mutant α1(X) chain
Bowed legs
Ulna bone
Early diagnosis

ABSTRACT

To evaluate the clinical-phenotypic characteristics of Schmid metaphyseal chondrodysplasia (SMCD) inflicted by a novel missense mutation of COL10A1 gene: c.2020G > A; p.Gly674Arg.

A female child aged about 3 yrs. and 8 months was subjected to Radiograph test to validate the symptoms of SMCD. The polymorphism analysis by the next-generation sequencing (NGS) was performed using the peripheral blood DNA samples of the patient and other family inmates, including, the younger male sibling. The effect of the mutation on the non-collagenous carboxyl-terminal (NC1) domain of collagen X was studied using the SWISS-MODEL online server for trimer modelling; PROSA and PROCHECK-Ramachandran plot for structural validation; Mean Square Plot (RMSF) for structural rigidity.

Radiograph examination of lower limbs confirmed the bowed legs in both the patient and her younger brother (study groups). The inheritance of the novel missense mutation of COL10A1: c.2020G > A; p.Gly674Arg (at chromosome-6q22.1) was confirmed in the study groups from the SMCD-affected mother. The extended interactions of the mutant-Arg674 with the Ser552 and Phe589 (β strand B) in the NC1 domain of α1(X) chain monomer is more likely to intervene its trimer formation by weakening the structural rigidity of the crucial strand H compared to its wild type. This plausibly deters the collagen X synthesis inflicting the bowed legs with the altered distal ulna bone morphology in the study groups.

The inheritance of COL10A1 mutation: c.2020G > A; p.Gly674Arg has inflicted the SMCD with the characteristic bowed legs in the study groups. Radiograph and NGS could be a valid diagnostic module to initiate the treatment of SMCD.

1. Introduction

Schmid metaphyseal chondrodysplasia (SMCD; OMIM #156500) is an autosomal dominant hereditary chondrodysplasia inflicted by the heterozygous mutations in the COL10A1 gene located at the chromosome 6q21-6q22.3 (Bateman et al., 2005; Al Kaissi et al., 2018). The clinical manifestations of SMCD are noticeable only after the second year of disease progression characterized by short-limbed dwarfism, bowed legs, and waddling gait (Al Kaissi et al., 2018). To confirm the incidence of SMCD, the radiography test and genome analysis for the COL10A1 mutation have been performed widely on the patients (Al Kaissi et al., 2018; Park et al., 2015; Hu et al., 2015).

The radiography analysis includes irregular acetabular roofs, enlarged capital femoral epiphyses, coxa vara, genu varum, metaphyseal irregularities with fraying and splaying in the knee, ankle, and wrist (Park et al., 2015; Cammarata-Scalisi et al., 2019). COL10A1 gene is comprised of 3 exons that encode the α1(X) chains of type X collagen, which is the short-chain collagen that regulates the hypertrophic chondrocytes of growth plate cartilage (Shen, 2005; Ho et al., 2007). Type X collagen is a homo-trimeric molecule made of three α1(X) chains with which each chain comprised of two non-collagenous globular domains at both the amino-terminal (NC2) and carboxyl-

* Corresponding authors at: Department of Endocrinology and Metabolism, Genetics, Henan children's hospital (Children's hospital affiliated to Zhengzhou University), Longhuwaihuan Road, Zhengzhou New District, Zhengzhou 450003, China.
E-mail addresses: haiyanwei2009@163.com (H.-Y. Wei), drsakbiomed1727@outlook.com (S.A. Kumar).

https://doi.org/10.1016/j.bonr.2019.100240
Received 27 September 2019; Received in revised form 9 December 2019; Accepted 12 December 2019
Available online 13 December 2019

terminal (NC1) ends (Warman et al., 1993; Bogin et al., 2002). With the NC1 domain being highly prone to get infused with the deleterious mutations (Bateman et al., 2005; Chan and Jacenko, 1998), to date, there are 54 COL10A1 mutations have been recorded according to the Human Gene Mutation Database (http://www.hgmd.cf.ac.uk/ac/all.php) within which the missense, nonsense, and frameshift mutations are noticeable among the SMCD-affected patients (Bateman et al., 2005; Park et al., 2015; Woelfle et al., 2011). Irrespective of these earlier recorded gene mutations, our genome analysis on the SMCD-affected female child and her younger male sibling has confirmed the inheritance of a novel missense gene mutation, c.2020G > A with the heterozygous substitution of glycine replaced by arginine in the 674th codon of COL10A1 from the SMCD-affected mother. Concomitantly, the modified structural characteristics of the α1(X) chain of collagen X mediated by this novel mutation, along with the other deleterious clinical symptoms, especially the bowed legs stature, and the cupping and fraying of ulna have been recorded in this study to facilitate the clinicians for a better understanding of the SMCD disease progression and its associated treatment.

2. Materials and methods

2.1. Background of the SMCD-affected child and the follow-up procedures

A 3 years and 8 months old girl child got admitted at the Genetics Out-patient Department, Henan children's hospital (Children's hospital affiliated to Zhengzhou University), China with phenotypic characteristics such as short-limbed dwarfism, bowed legs, waddling gait and genu varum for the examination of SMCD. The female child patient was born after 40 weeks of gestation to the nonconsanguineous parents whose mother and her younger male sibling showed noticeable clinical symptoms of SMCD. Based on the clinical inquiry with the patient's mother, we found that none of the other close family relatives has shown such clinical symptoms of SMCD. Earlier, the patient was misdiagnosed and treated for the vitamin D deficiency while she was a year and 8 months old at the local hospital in China which may be due to the waddling gait characteristics of SMCD mimicking the clinical symptoms of a vitamin D-deficient child. Since the child didn't show any sign of improvement in her clinical symptoms even after her treatment for the vitamin D deficiency for two years. She has been further examined by our physicians at the Genetics Out-patient Department of Henan children's hospital (Children's hospital affiliated to Zhengzhou University) with which the laboratory tests, and as well as the radiographic examination and the genome analysis have confirmed the incidence of SMCD on the female child patient. Concomitantly, the clinical diagnosis of the same module was performed on the patient's younger male sibling aged 1 year and 5 months old accompanied with the polymorphism analysis on the patient's biological parents to confirm the inheritance of SMCD in the affected child. The study was approved by the Ethics Committee of Henan Children's Hospital (Children's hospital affiliated to Zhengzhou University). Informed consent was obtained from the patient and her younger brother (the study groups), and as well as from their parents (as guardians) as the proof of acknowledgement to take part in the study.

2.2. Gene polymorphism analysis by the next-generation gene sequencing

DNA was extracted from the peripheral blood collected from the patient as well as from the patient's family using the QIAamp DNA Blood Midi kit (Qiagen, Hilden, Germany). Exome enrichment was performed using the Seq Cap EZ Exome Probes v3.0 (Roche, Switzerland). Polymorphic variants that showed > 0.5% allele frequency in general populations were filtered out (based on the database of 1000 genomes sequencing project: http://www.1000genomes.org/). The SIFT, PolyPhen, MutationTaster and M-CAP were used to assist in predicting the functional impact of identified missense variants (Adzhubei et al., 2010; Schwarz et al., 2014; Jagadeesh et al., 2016; Vaser et al., 2016).

Oligonucleotides flanking the genomic locations of identified variants were designed using the Primer3Plus browser. Polymerase chain reactions (PCR) was performed with the following primers: 5′- TTGTT AGTGCCAACCAGGGG-3′ and 5′- CTGCTCACTTTTCAGGGGGA-3′. PCR products were sequenced bi-directionally using Big Dye Terminator chemistry v3.1 and sequenced using an ABI 3730XL sequencer (Applied Biosystems/Life Technologies, Carlsbad, CA, USA). Sequences were reviewed manually using Mutation Surveyor (SoftGenetics, State College, PA) and compared to the wild type reference sequences of COL10A1 (NM_000493).

2.3. Evaluation of the structural changes of the mutant-collagen X protein structure compared with its wild type in an in-silico setup

Collagen X protein sequence was downloaded from Uniprot Database (Bairoch and Apweiler, 1997) (ID: Q03692) which basically exists in trimeric form. Structure-based search from the Protein Data Bank (Berman, 2008) listed only the monomeric structure instead of the trimer. Thus, to model the trimer, we considered SWISS-MODEL online server (Schwede et al., 2003) wherein wild type collagen X protein was considered as the query sequence. Of the listed templates, the 3D structure with better query coverage and amino acid identity was considered as the template and the 3D model was generated. Furthermore, mutant collagen protein was modelled in which the Gly674 was replaced with positively charged Arg674 in the sequence and was further considered for 3D modelling. Both the wild and the mutant structures were validated using ProSA-Web (Wiederstein and Sippl, 2007) and PROCHECK-Ramachandran Plot (Laskowski et al., 1993). To understand the effect of the mutation on protein flexibility, we have chosen the CABS-flex 2.0 online server (Kuriata et al., 2018) that has been widely acknowledged for its efficacy as a tool to study the fast simulations of protein structure flexibility. The monomeric subunit of the modelled wild and the mutant collagen proteins were submitted while keeping the parameters default. The Root Mean Square Fluctuation Plot (RMSF) from the result files were considered for further analysis.

3. Results

3.1. Clinical background with the follow-up outcomes of the patient and the younger male sibling

During the early stages of examination, the patient was diagnosed with short-limbed dwarfism, bowed legs, waddling gait, and genu varum. The patient was recorded with an average height measured about 85.2 cm (−3.7 SD) at the age of 3 years and 8 months old (Fig. 1D). Blood-serum level measurements showed higher concentrations of 25-hydroxyvitamin D (> 70 ng/ml) which may be due to vitamin D treatment upon the misdiagnosis of rickets over SMCD at the local hospital. Furthermore, serum level measurements of calcium, phosphorus, alkaline phosphatase, calcitonin, and parathyroid hormone didn't show any sign of abnormalities on the patient (data not shown). The anteroposterior lower limb radiograph has confirmed the bowed legs stature in the patient (Fig. 1B).

A follow-up examination of the SMCD-linked clinical phenotype symptoms was carried out on the proband's younger male sibling (aged 1 year and 5 months) who showed short-limbed dwarfism, bowed legs, waddling gait and genu varum alike the patient. The bowed legs stature of the anteroposterior lower limb of the male sibling has been shown in Fig. 1C. Lateral cervical spine vertebral bodies (C1 to C7) structure was diagnosed normal with which the dens (odontoid process) of the C1 vertebral body was axially centered with no abnormalities detected in the C1 and C2 stability accompanied with the symmetrical posterior and anterior vertebral line, and the symmetrical spinous process and

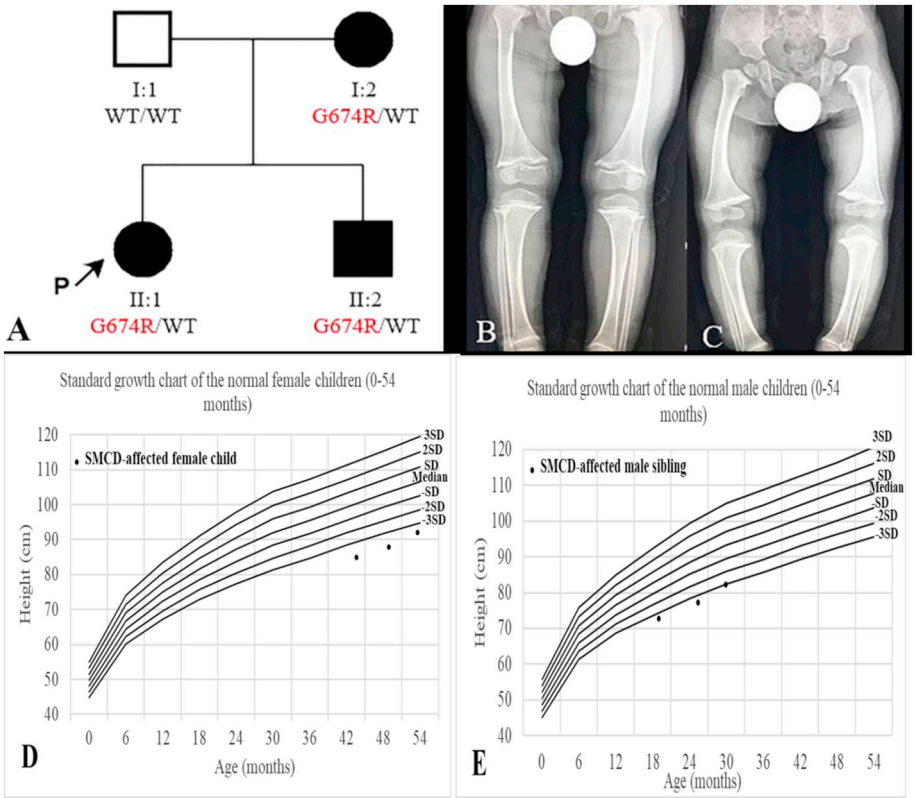

Fig. 1. Familial tree and clinical characteristics of the Schmid Metaphyseal Chondrodysplasia (SMCD)-affected family: A, Pedigree tree of the SMCD-affected family:Symbols colored black denotes the SMCD-affected individuals; P, denotes the SMCD-affected female child patient; I:1 and I:2 implies the biological father and mother of the children; II.1 and II.2 implies the daughter and the son of the parents. B and C, Anteroposterior lower limb radiograph of the SMCD-affected female child patient (B) and the younger male sibling (C). D and E, plotting of height measurement values of the SMCD-affected female child patient (D) and the younger male sibling (E) recorded at different age points (in months) marked using dotted circles on the standard growth line chart.

spinolaminal lines in the female proband and male sibling (Fig. 2A and B). The skeleton structure of the lumbar vertebral bodies (L1 to L5) appeared normal with the appropriate intervertebral disc space, spinous process and inferior articular process in both the female proband and the male sibling (Fig. 2C and D). Though the phalanges (distal, middle, and proximal fingers) skeleton structure, including, the metacarpals were diagnosed normal; cupping and fraying of the distal metaphyseal edges of the ulna was detected in both the female proband and the male sibling (Fig. 3 A, B). However, the male sibling showed less severity in the clinical symptoms of SMCD with the average height measured about 72.8 cm (−3.1 SD) in 20 months of age (Fig. 1E), and with the normal 25-hydroxyvitamin D levels (data not shown). A comparative growth chart of the patient and her younger brother monitored over a period of 10 months with the other normal children has been shown in Fig. 1D and E. With the patient's mother who showed abnormal phenotypic characteristics alike, her daughter was recorded with an average height ranging about 145 cm (−2.9 SD) compared to her normal healthy partner (the patient's father) with an average height measured about 170 cm (−0.44 SD). The family tree has been shown in Fig. 1A. Furthermore, genome analysis of the inflicted mutations associated with the SMCD on the patient and the affected immediate family members that includes both her younger brother and the mother has confirmed the incidence of SMCD. Alternatively, compared with the other earlier recorded clinical evidence of SMCD, we found both the patient and her younger sibling showed obvious skeletal lesions during the early stages of the development of SMCD (Bateman et al., 2005; Cammarata-Scalisi et al., 2019; Goyal et al., 2019).

3.2. Polymorphic variants detected on the SMCD affected family by the next-generation sequencing

Next-generation sequencing was performed on the peripheral blood DNA samples isolated from the SMCD-affected female child patient, and as well as from the patient's younger male sibling and their biological parents. The detected polymorphic gene variants were prioritized and selected according to ACMG (American College of Medical Genetics and Genomics) guidelines. The diagrammatic representation of the next-generation sequencing results, including the detection of mutation (at the chromosome loci 6q22.1) in the NC1 domain of the patient and the family inmates have been shown in Fig. 4A. With the careful evaluation of the coding exons with its flanked introns by the PCR-direct sequencing, we spotted a novel missense mutation, c.2020G > A accompanied by the heterozygous amino acid substitution, p.Gly674Arg located in the NC1 domain of α1(X) chain of collagen X protein (Fig. 4A). This mutation hasn't been reported in any of the recommended genomic databases generated by the dbSNP such as the 1000 Genome Project, the Exome Variant Server, and the NHLBI (National Heart, Lung and Blood Institute) Exome Sequencing Project. Based on these evaluation-based scores created by Polyphen-2 (score at 1.00), SIFT (score at 0.006), Mutation Taster (score at 1), and M-CAP (0.317), we speculate that this novel missense mutation c.2020G > A; p.Gly674Arg at the NC1 domain could be deleterious as the glycine amino acid residue at 674 positions is the highly conserved residue since the evolution of organisms begins from Zebrafish to humans (Fig. 4B) (Warman et al., 1993; Bogin et al., 2002; Chan and Jacenko, 1998). With the familial genome analysis performed using the same methodology and genomic tools discussed above, our study has confirmed inheritance of the missense mutation: c.2020G > A; p.Gly674Arg in the patient's younger male sibling from the SMCD-affected mother (Fig. 4A). Furthermore, based on the comparison of the SMCD-affected female child, including the patient's male sibling and the mother with the healthy-control father (Fig. 4A), we propose the c.2020G > A; p.Gly674Arg mutation of the COL10A1 gene could be detrimental to the patients.

3.3. Structural alterations of the α1(X) chain of collagen X and its effect on the collagen X protein structure inflicted by the p.Gly674Arg mutation

During the template search in SWISSMODEL online server, wild type scored a query coverage of 24 percentage (residues 521–680) with a 100 percentage amino acid identity with the human collagen X NC1

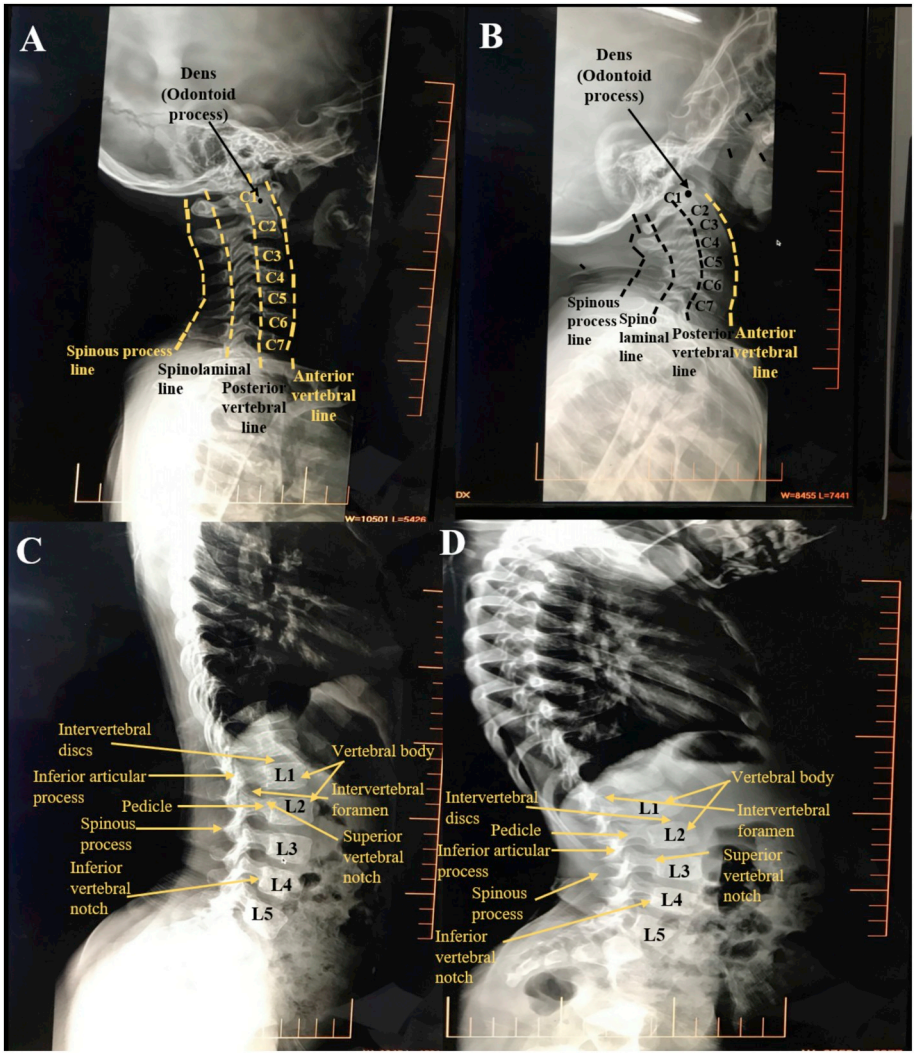

Fig. 2. Structural skeleton evaluation of the lateral cervical spine vertebrae and lumbar vertebrae by radiograph imaging in the Schmid Metaphyseal Chondrodysplasia (SMCD)-affected female child and the younger male sibling. A and B, A normal skeleton structure of the seven cervical vertebral spine bodies marked as C1 to C7 with the axially centered dens (odontoid process) structure (marked using black dot), and the unaffected spinous process with the symmetrical spinolaminal, posterior and anterior vertebral lines in the SMCD-affected female child (A) and her younger male sibling (B). C and D, A normal skeleton structure of the five lumbar vertebral bodies marked as L1 to L5 with the unaffected intervertebral disc space; intervertebral foramen; spinous and the inferior articular process in the SMCD-affected female child (C) and the male sibling (D).

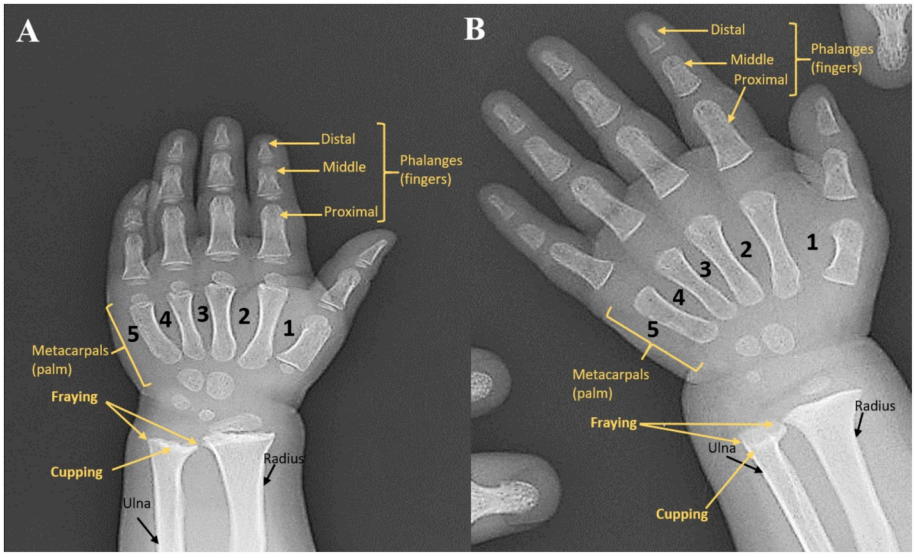

Fig. 3. Skeleton characteristics of phalanges (fingers), especially the metacarpals, ulna and the radial bone of the Schmid Metaphyseal Chondrodysplasia (SMCD)-affected female child and the younger male sibling by radiograph imaging. A and B, A normal skeleton features of the distal, middle, proximal and metacarpals (palm) of the SMCD-affected female child and the male sibling; cupping and fraying of the distal metaphyseal ulna bone edges of the SMCD-affected female child (A) and the male sibling (B).

trimer (PDB ID: 1GR3) (Dassault Systèmes, 2019). This template was considered for the generation of collagen X NC1 trimer (Fig. 4C). Regarding mutant, the query coverage remained the same, nevertheless, the identity was 99.38 percentage after the substitution of glycine with arginine. Structure validation through ProSA-Web online server confirms a better model quality with the value below zero for the window size of 40 (Fig. 5A and B). As per the PROCHECK-Ramachandran plot analysis, 94.6% residues are in most favoured regions; 4.5% in

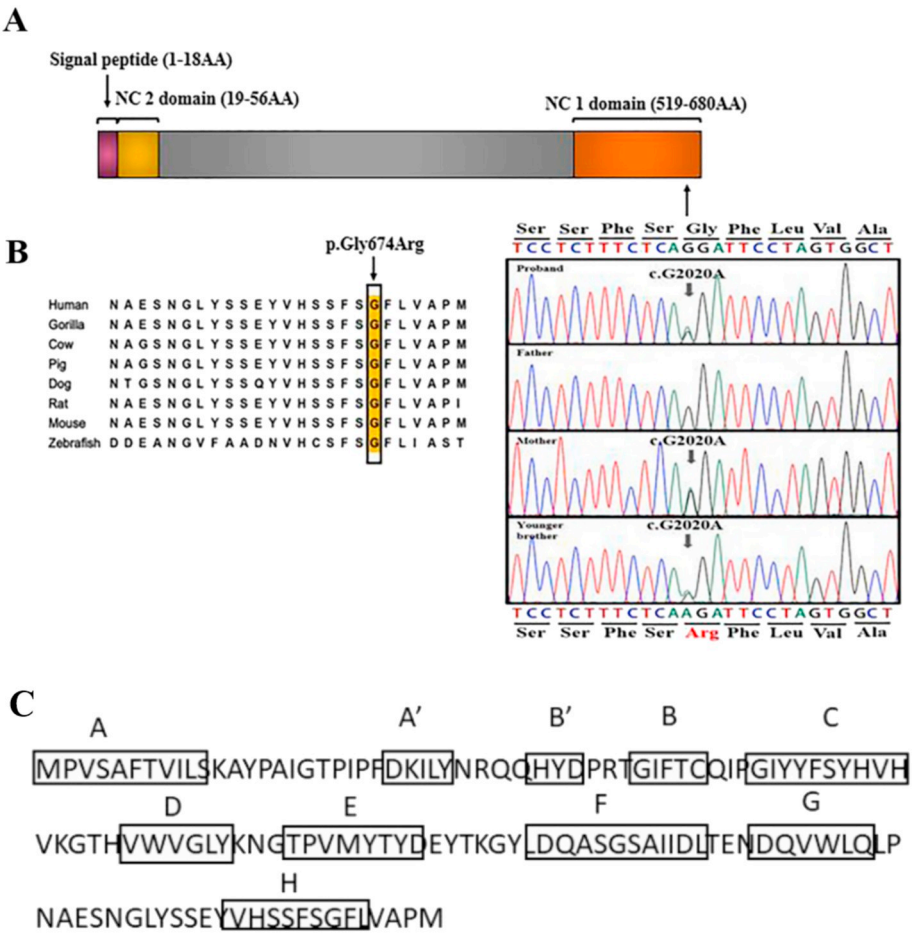

Fig. 4. Characterization of polymorphic variants by the next-generation sequencing and the template peptide sequence of the human collagen X- non-collagenous carboxyl-terminal (NC1) domain:A, a novel missense mutation, c.2020G > A; p.Gly674Arg detected at the NC1 domain of the COL10A1 gene over at the non-collagenous amino-terminal (NC2) domain in the Schmid Metaphyseal Chondrodysplasia (SMCD)-affected female child (proband) followed by the healthy father, and the SMCD-affected mother and the younger brother. B, a diagrammatic representation of the highly conserved glycine residue in the 674th codon of the COL10A1 gene of higher mammals shown in the following chronological order of hierarchy (from top to bottom): Humans; Gorilla; Cow; Pig; Dog; Rat; Mouse, and Zebrafish. C, the orientation of the peptide sequence organized in the alphabetical order from A-H of the beta-strands of the NC1 domain of α1(X) chain monomer.

additional allowed regions and 0.9% in generously allowed regions (Fig. 5C and D). There are no residues within the disallowed region, thus, confirming it to be the best-modelled structure. A similar report was observed for the mutant.

The modelled trimeric wild and the mutant collagen X proteins were considered for hydrogen bond analysis using the Discovery Studio 2019 client (Bogin et al., 2002). In the wild type NC1 domain of the α1(X) chain monomer of collagen X, Gly674 from β strand H interacts with Phe554 (β strand A) and Tyr598 (β strand C). While in the mutant α1(X) chain monomer, the Arg674 interacts with Ser552, Phe554 (β strand A) and Phe589 (β strand B). Following which an overall shift in the hydrogen bonding pattern was observed between the wild and the mutant (Fig. 5C and D). Concomitantly, the RMSF plot of the wild and the mutant proteins were analysed. It was observed that in wild type, Gly674 brings rigidity to the loop I which is following strand A and also the loop preceding the strand H. Furthermore, the strand H is rigid in wild type that contradicts its flexible stature in the mutant type (Fig. 6A and B).

4. Discussion

The study has reported a novel missense mutation c.2020G > A with the heterozygous substitution of glycine with arginine, p. Gly674Arg in the NC1 domain of α1(X) chain of collagen X at the chromosome loci 6q22.1 (Fig. 4A); that triggered the incidence of SMCD in the female child patient. Also, the inheritance of this novel COL10A1 gene mutation from the SMCD-affected mother (as a carrier) has been confirmed in the patient's younger male sibling (Fig. 4A), who were diagnosed with clinical symptoms like short-limbed dwarfism, bowed legs, waddling gait, and genu varum. The missense mutation inflicted by the glycine replacement with arginine in the 674th codon of COL10A1 gene encoding the NC1 domain of the α1(X) chain could intervene the collagen X structure and function by attenuating its trimer formation initiated by the three α1(X) chain monomers (Warman et al., 1993; Bogin et al., 2002; Chan and Jacenko, 1998). Earlier evidence has shown the residues Ala553, Ile557, Leu575, val621, Ile641, Phe675 and Ala678 to be directly associated with the intact packing of the α1(X) chains-trimer supported by the Pro550, Val551, Phe675 and Pro679 residues that forms the hydrophobic plug at the base of the NC1 trimer generating a firm collagen X protein structure (Marks et al., 1999). Having confirmed the stable interaction of both the wild-Gly674 and mutant-Arg674 amino acid residues with the Phe554 residue, which is proximal to the Ala553 residue (Fig. 5C and D); we explored the extended interactions of Arg674 with the Ser552, and Phe589 (β strand B) over the Gly674 interactions with Tyr598 (β strand C) (Fig. 5C and D). Also, the residue Phe675 which is crucial for the compact trimer packing as well as for the hydrophobic plug formation turns out to be a flexible one in the mutant α1(X) chains of the collagen X protein compared with its wild type (Figs. 5B and 6A, B). These structural changes inflicted by the missense p. Gly674Arg mutation has indeed affected the overall rigidity of the α1(X) chain monomer (Fig. 6B) that plausibly interlude its assembly as a trimer to generate a compact collagen X structure. There could be a direct correlation between the heterozygous p.Gly674Arg mutation and the adverse clinical symptoms like the bowed legs in the SMCD-affected female child and her younger brother preceded by the effaced collagen X structure and function (Bogin et al., 2002; Chan and Jacenko, 1998; Stratakis et al., 1996). Also, the disturbed rigidity of the α1(X) chain monomer of collagen X could precede the cupping and fraying of the distal metaphyseal edges of ulna despite the phalanges (fingers), metacarpals, lateral cervical

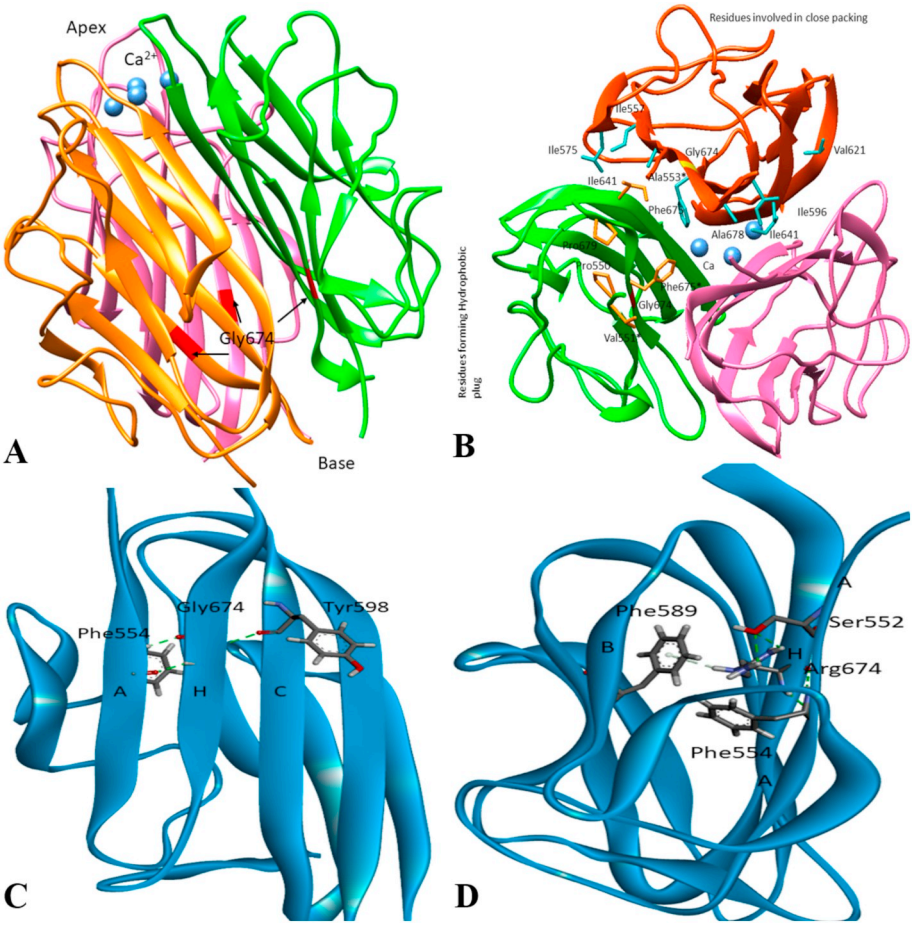

Fig. 5. Structural characteristics of the α1(X) chain of non-collagenous carboxyl-terminal (NC1) trimer and the effect of mutant-Arg674 residue on the NC1 domain of α1(X) chain compared with its wild type with Gly674 residue. A, a modelled NC1 trimer with highlighted Apex and Base region having intact Ca^{2+} cluster at the apex. B, chain (marked in green) with the hydrophobic plug forming residues at the base of the monomeric subunit. Phe675 being an active member of the hydrophobic plug is proximal to Gly674 (marked by Asterix * symbol). Residues Val551 and Ala553 are highlighted by Asterix * symbol which flanks Ser552 and Phe554 and forms hydrogen bonds in the wild and mutant protein. C, in the wild type NC1 domain of α1(X) chain, Gly674 from strand H showed hydrogen bonds with Phe554 and Tyr598 from strand A and C respectively. D, in the mutant NC1 domain of α1(X) chain, Arg674 (strand H) showed strong hydrogen bond formation with Ser552 and Phe554 of strand A. Additionally, there is a weak hydrogen bond formation observed between Phe589 of strand B and Arg674.

spine, dens (odontoid process), and the lumbar vertebrae skeleton remained unaffected in the SMCD-affected female child and the male sibling (Figs. 3A,B and 2A-D) (Bairoch and Apweiler, 1997). Since the SMCD clinical symptoms overlap with the other similar clinical symptoms of achondroplasia and rickets (Goyal et al., 2019; Higuchi et al., 2016; Daugherty, 2017), we recommend the differential diagnosis of SMCD to all the clinicians to prevent any misdiagnosis. The differential diagnosis of SMCD can be achieved by performing the diagnosis at various levels on the patients. At the first level, a thorough examination of the patient's clinical symptoms, including their family members,

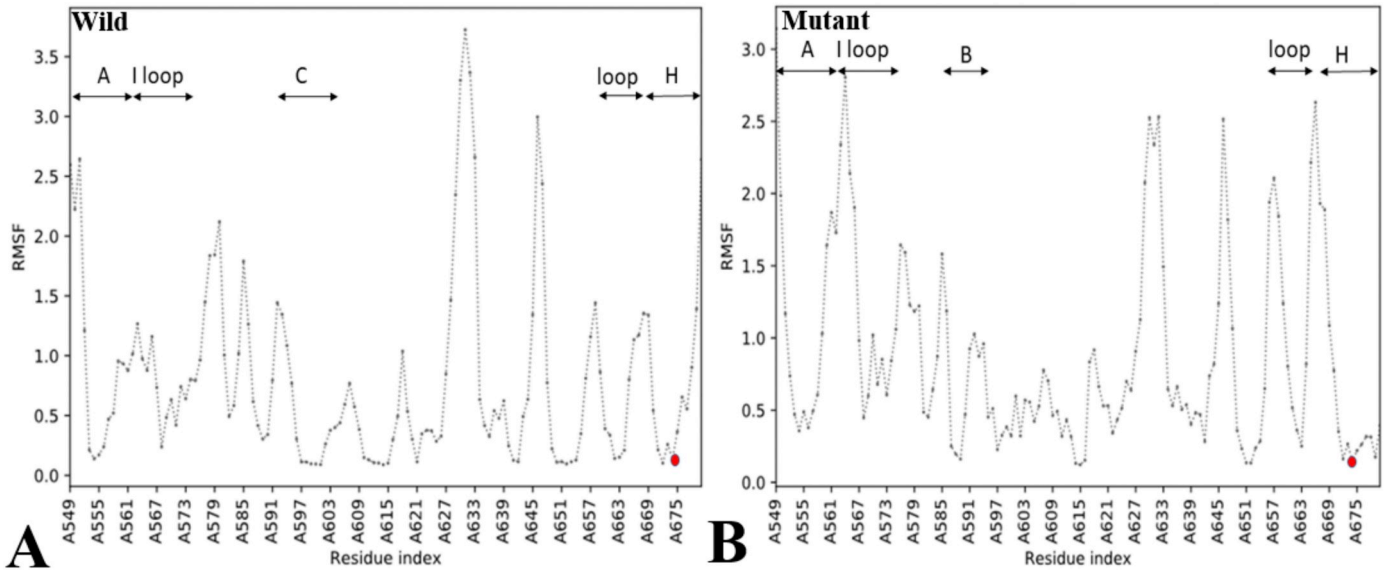

Fig. 6. Determination of structural rigidity of the mutant α1(X) chain monomer of NC1 domain compared with its wild type by the Root Mean Square Fluctuation (RMSF) plot: A, RMSF plot of wild monomer; strand H, A and C along with loop I and the loop preceding strand H are rigid in wild type. B, RMSF plot of mutant monomer; strand H, A and B along with loop I and the loop preceding strand H are flexible in mutant type. Gly674 residue has been marked using the red colour circle in both A and B plots.

must be carried out diligently. The second level of radiography examination must be performed cautiously with an in-detail skeletal survey of the anteroposterior lower limbs, lateral cervical spine vertebrae, lumbar vertebral bodies, and phalanges to differentiate the patients with rickets showing similar phenotypic characteristics like the SMCD-affected children of the study (Figs. 1B and C, 2A-D, 3A,B). At the third-final level of examination, the polymorphism analysis must be performed diligently to categorize the SMCD-affected patients over the other patients with achondroplasia and rickets-based on the inheritance of the polymorphic gene variants. Despite the noticeable improvements eventually seen in the abnormal body skeleton structure corrected by the surgical interventions in the SMCD patients, a majority of the patients still retain their short stature with coxa vara (Stratakis et al., 1996; Makitie et al., 2005). Surgical intervention is employed to rectify the symptomatic deformity detected in the SMCD affected patients (Stratakis et al., 1996).

In conclusion, our study is the first to report the inheritance of SMCD in the Chinese family inflicted by the novel missense mutation, c.2020G > A; p.Gly674Arg, affecting the structural rigidity of the α1(X) chain monomer that is more likely to intervene its trimer formation disrupting the collagen X protein structure and function. We have also found a direct correlation between the disturbed genotypic and phenotypic characteristics, especially the bowed legs in the SMCD-affected Chinese family. In additional to the other clinical diagnosis tests, we also suggest the Radiograph test together with the next-generation gene sequencing to be crucial to initiate the early diagnosis and treatment of SMCD.

Funding

The research study doesn't receive any financial aid from any of the funding agencies, including the commercial sectors, public, or non-profit organizations at any time point of the study.

Declaration of competing interest

The authors declare that they have no known competing financial interests or personal relationships that could have appeared to influence the work reported in this paper.

Acknowledgement

We would like to deeply express our gratitude to Dr. Hai-Yan Wei, the Director of the Endocrinology and Metabolism, Genetics, Henan Children's hospital (Children's Hospital Affiliated to Zhengzhou University), China who helped us to conduct the whole clinical follow-up examination on the SMCD-affected patient and the family inmates. Also, we would thank the patient's parents, staff head nurse and other lab technicians who showed extreme co-operation for this study with utmost diligence and integrity.

References

Adzhubei, I.A., Schmidt, S., Peshkin, L., Ramensky, V.E., Gerasimova, A., Bork, P., et al., 2010. A method and server for predicting damaging missense mutations. Nat. Methods 7 (4), 248–249.

Al Kaissi, A., Ghachem, M.B., Nabil, N.M., Kenis, V., Melchenko, E., Morenko, E., et al., 2018. Schmid's type of metaphyseal chondrodysplasia: diagnosis and management. Orthop. Surg. 10 (3), 241–246.

Bairoch, A., Apweiler, R., 1997. The SWISS-PROT protein sequence database: its relevance to human molecular medical research. J Mol Med (Berl) 75 (5), 312–316.

Bateman, J.F., Wilson, R., Freddi, S., Lamande, S.R., Savarirayan, R., 2005. Mutations of COL10A1 in Schmid metaphyseal chondrodysplasia. Hum. Mutat. 25 (6), 525–534.

Berman, HM., 2008. The Protein Data Bank: a historical perspective. Acta Crystallogr A. 64 (Pt 1), 88–95. https://doi.org/10.1107/S0108767307035623.

Bogin, O., Kvansakul, M., Rom, E., Singer, J., Yayon, A., Hohenester, E., 2002. Insight into Schmid metaphyseal chondrodysplasia from the crystal structure of the collagen X NC1 domain trimer. Structure 10 (2), 165–173.

Cammarata-Scalisi, F., Matysiak, U., Velten, T., Callea, M., Araque, D., Willoughby, C.E., et al., 2019. A venezuelan case of Schmid-type metaphyseal chondrodysplasia with a novel mutation in COL10A1. Molecular syndromology 10 (3), 167–170.

Chan, D., Jacenko, O., 1998. Phenotypic and biochemical consequences of collagen X mutations in mice and humans. Matrix biology : journal of the International Society for Matrix Biology 17 (3), 169–184.

Dassault Systèmes, 2019. BIOVIA BW, Release 2019. BIOVIA Pipeline Pilot. Dassault Systèmes, San Diego.

Daugherty, A., 2017. Achondroplasia: etiology, clinical presentation, and management. Neonatal network : NN 36 (6), 337–342.

Goyal, M., Gupta, A., Choudhary, A., Bhandari, A., 2019. Schmid type metaphyseal chondrodysplasia with a novel COL10A1 mutation. Indian J. Pediatr. 86 (2), 183–185.

Higuchi, S., Takagi, M., Shimomura, S., Nishimura, G., Hasegawa, Y., 2016. A Japanese familial case of Schmid metaphyseal chondrodysplasia with a novel mutation in COL10A1. Clinical pediatric endocrinology : case reports and clinical investigations : official journal of the Japanese Society for Pediatric Endocrinology 25 (3), 107–110.

Ho, M.S., Tsang, K.Y., Lo, R.L., Susic, M., Makitie, O., Chan, T.W., et al., 2007. COL10A1 nonsense and frame-shift mutations have a gain-of-function effect on the growth plate in human and mouse metaphyseal chondrodysplasia type Schmid. Hum. Mol. Genet. 16 (10), 1201–1215.

Hu, X., Zhang, X., Li, Y., Lou, P., Li, X., Jiang, L., 2015. A novel COL10A1 mutation in a Chinese pedigree with Schmid type metaphyseal chondrodysplasia. Clin. Lab. 61 (3–4), 227–233.

Jagadeesh, K.A., Wenger, A.M., Berger, M.J., Guturu, H., Stenson, P.D., Cooper, D.N., et al., 2016. M-CAP eliminates a majority of variants of uncertain significance in clinical exomes at high sensitivity. Nat. Genet. 48 (12), 1581–1586.

Kuriata A, Gierut AM, Oleniecki T, Ciemny MP, Kolinski A, Kurcinski M, et al. CABS-flex 2.0: a web server for fast simulations of flexibility of protein structures. Nucleic Acids Res.. 2018;46(W1):W338-W43.

Laskowski, R.A., Macarthur, M.W., Moss, D.S., Thornton, J.M., 1993. PROCHECK: a program to check the stereochemical quality of protein structures. J. Appl. Crystallogr. 26, 283–291.

Makitie, O., Susic, M., Ward, L., Barclay, C., Glorieux, F.H., Cole, W.G., 2005. Schmid type of metaphyseal chondrodysplasia and COL10A1 mutations–findings in 10 patients. Am. J. Med. Genet. A 137A (3), 241–248.

Marks, D.S., Gregory, C.A., Wallis, G.A., Brass, A., Kadler, K.E., Boot-Handford, R.P., 1999. Metaphyseal chondrodysplasia type Schmid mutations are predicted to occur in two distinct three-dimensional clusters within type X collagen NC1 domains that retain the ability to trimerize. J. Biol. Chem. 274 (6), 3632–3641.

Park, H., Hong, S., Cho, S.I., Cho, T.J., Choi, I.H., Jin, D.K., et al., 2015. Case of mild Schmid-type metaphyseal chondrodysplasia with novel sequence variation involving an unusual mutational site of the COL10A1 gene. European journal of medical genetics 58 (3), 175–179.

Schwarz, J.M., Cooper, D.N., Schuelke, M., Seelow, D., 2014. MutationTaster2: mutation prediction for the deep-sequencing age. Nat. Methods 11 (4), 361–362.

Schwede, T., Kopp, J., Guex, N., Peitsch, M.C., 2003. SWISS-MODEL: an automated protein homology-modeling server. Nucleic Acids Res. 31 (13), 3381–3385.

Shen, G., 2005. The role of type X collagen in facilitating and regulating endochondral ossification of articular cartilage. Orthodontics & craniofacial research 8 (1), 11–17.

Stratakis, C.A., Orban, Z., Burns, A.L., Vottero, A., Mitsiades, C.S., Marx, S.J., et al., 1996. Dideoxyfingerprinting (ddF) analysis of the type X collagen gene (COL10A1) and identification of a novel mutation (S671P) in a kindred with Schmid metaphyseal chondrodysplasia. Biochem. Mol. Med. 59 (2), 112–117.

Vaser, R., Adusumalli, S., Leng, S.N., Sikic, M., Ng, P.C., 2016. SIFT missense predictions for genomes. Nat. Protoc. 11 (1), 1–9.

Warman, M.L., Abbott, M., Apte, S.S., Hefferon, T., McIntosh, I., Cohn, D.H., et al., 1993. A type X collagen mutation causes Schmid metaphyseal chondrodysplasia. Nat. Genet. 5 (1), 79–82.

Wiederstein, M., Sippl, M.J., 2007. ProSA-web: interactive web service for the recognition of errors in three-dimensional structures of proteins. Nucleic Acids Res. 35 (Web Server), W407–W410.

Woelfle, J.V., Brenner, R.E., Zabel, B., Reichel, H., Nelitz, M., 2011. Schmid-type metaphyseal chondrodysplasia as the result of a collagen type X defect due to a novel COL10A1 nonsense mutation: a case report of a novel COL10A1 mutation. Journal of orthopaedic science : official journal of the Japanese Orthopaedic Association 16 (2), 245–249.